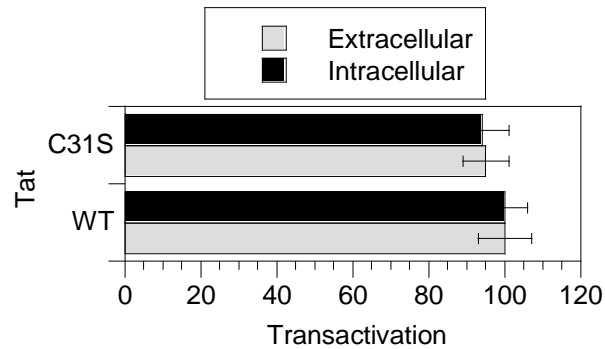
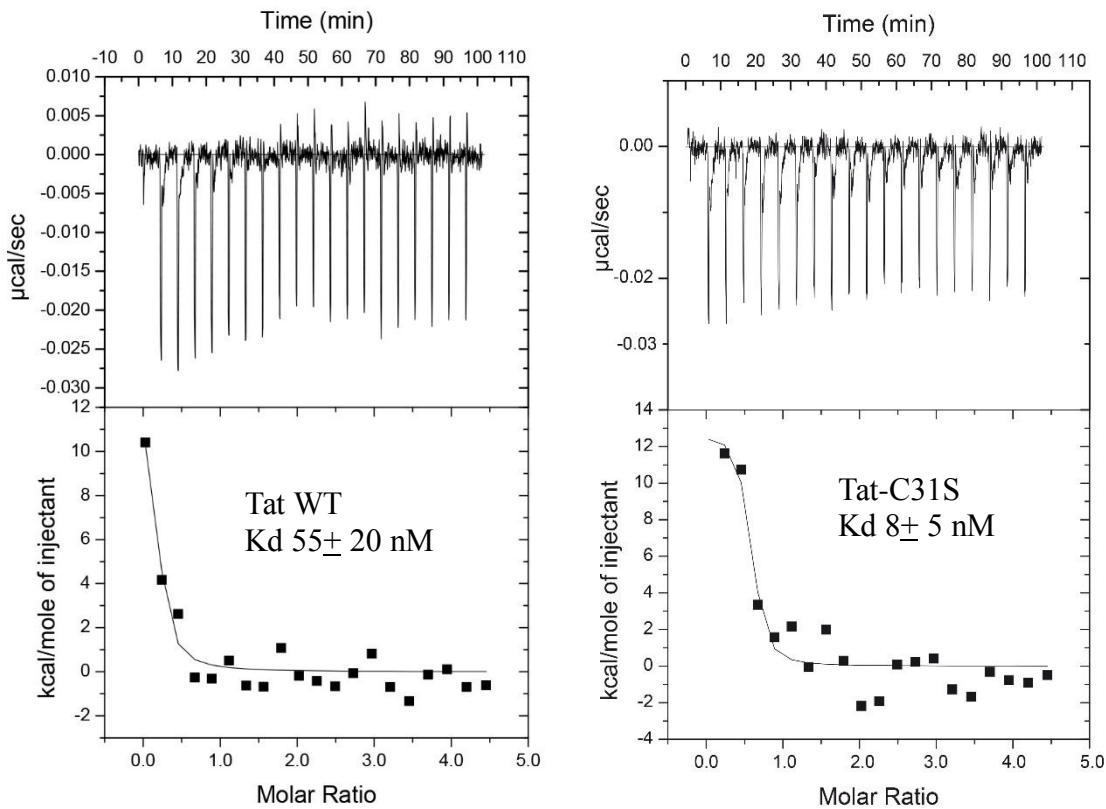


Supplementary Figure 1



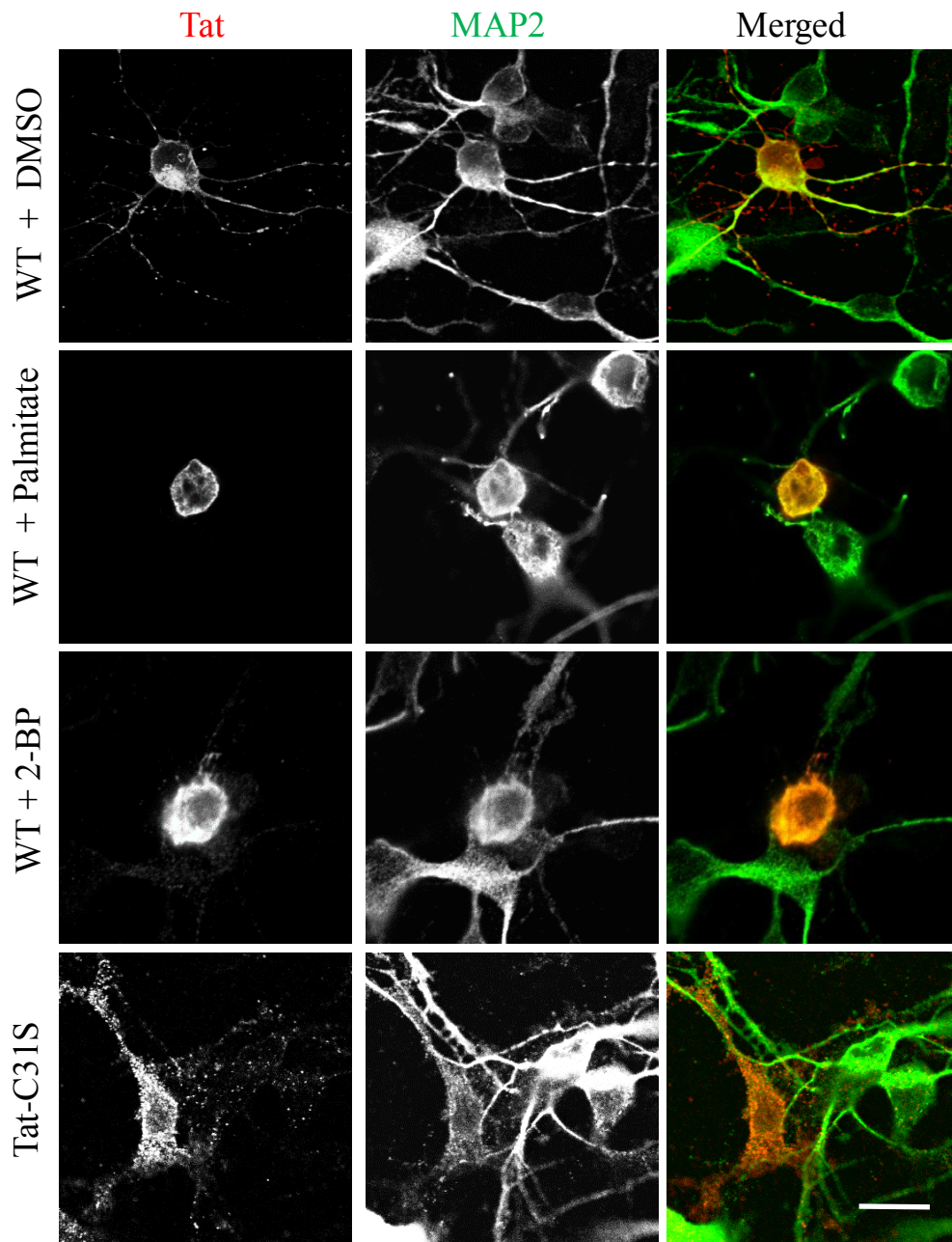
The C31S mutation does not affect Tat capacity to enter cells or its transcriptional activity. PC12 cells were cotransfected with a Tat vector (Intracellular), a vector expressing a Firefly gene under the control of an LTR promoter, a plasmid with a Renilla gene under a CMV promoter and a human cyclin T1 vector. When indicated (Extracellular), cells were not transfected with Tat but were treated with recombinant Tat, WT or C31S for 24 h. Luciferase activities were then assayed and transactivation is expressed as the Firefly/ Renilla ratio (%) compared to the corresponding control (Vendeville et al, 2004). Mean \pm SEM, n=4.

Supplementary Figure 2



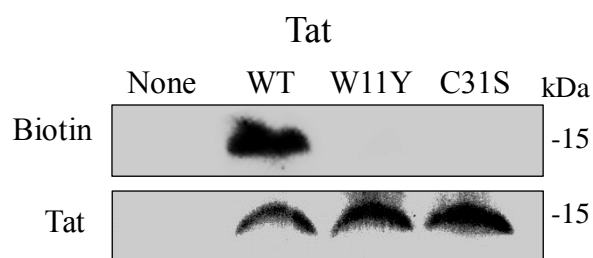
Interaction of Tat-C31S with PI(4,5)P₂ liposomes. Raw ITC data. Liposomes (PC/PG/PI(4,5)P₂ 75/20/5; 200 μM) were injected into 1 μM Tat WT or C31S (1 μM) in 150 mM NaCl, 50 mM Citrate, pH 7.3, and heat production was monitored. The heat resulting from buffer injection was subtracted from the binding curves. The Tat-PI(4,5)P₂ liposome interaction in NaCl buffer is exothermic ($\Delta H < 0$), while in KCl buffer it is endothermic ($\Delta H > 0$)¹. Mean \pm SEM (n=3).

Supplementary Figure 3



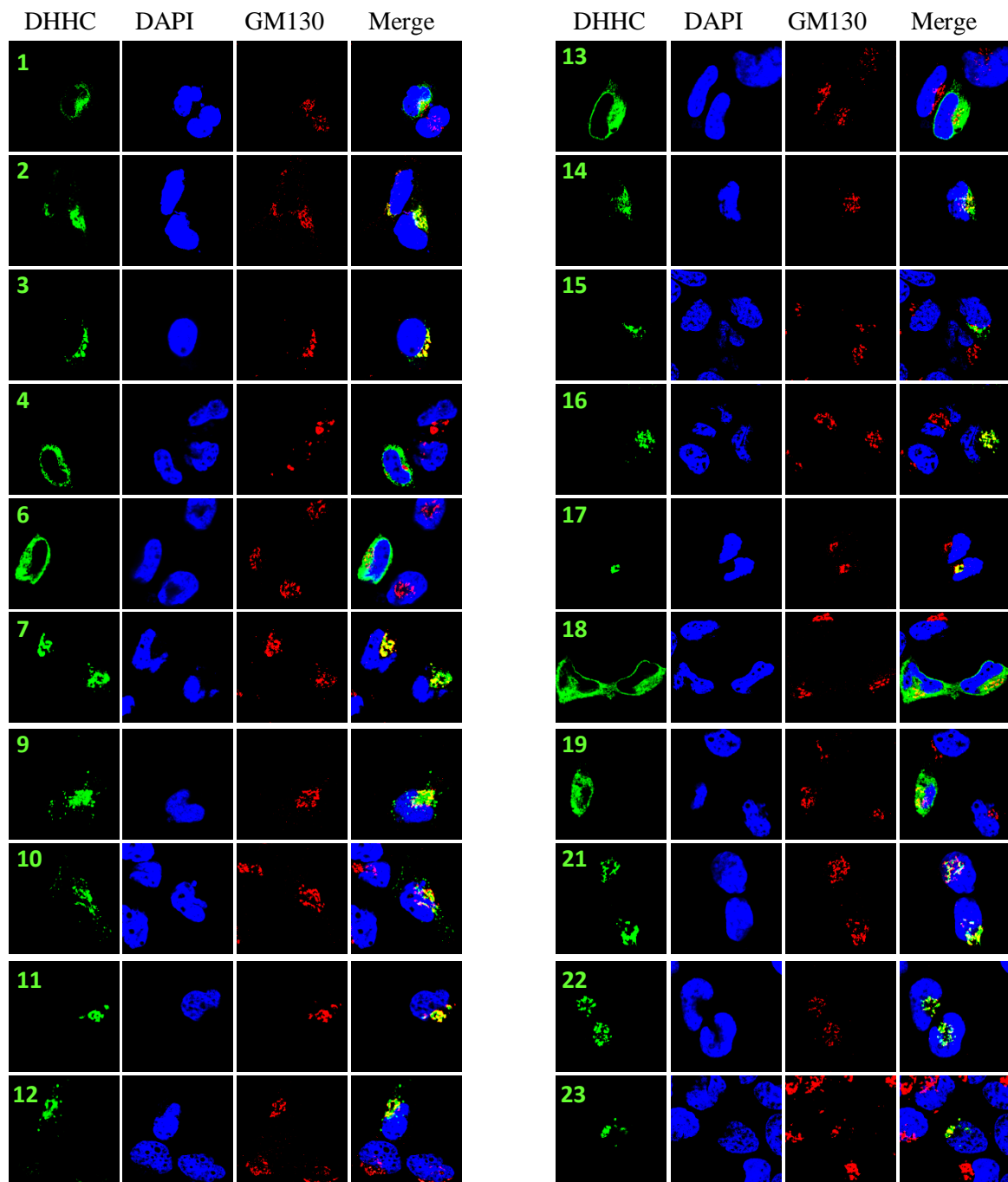
Tat palmitoylation is required for membrane association in primary neurons. Hippocampal neurons were transfected with a Tat vector. After 20h, when indicated, 50 μ M 2-BP, palmitate or solvent was added for 4 h. Neurons were then fixed for Tat and MAP2 (to confirm neuronal identity) immunostaining then imaged using a confocal microscope. Representative median optical sections are shown. Bar, 10 μ m. n=10.

Supplementary Figure 4

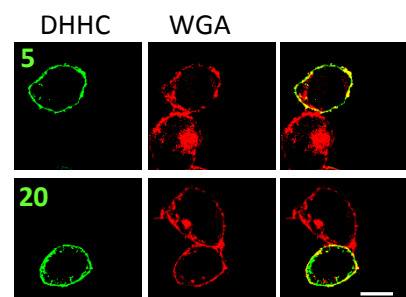


Exogenous Tat-C31S and Tat-W11Y are not palmitoylated. Jurkat cells were treated overnight with 100 μ M 17-ODYA and 50 nM Tat-His₆, WT, C31S or W11Y as indicated. After cell lysis, Tat-His₆ was isolated on Ni-NTA-agarose beads before click chemistry to attach biotin to 17-ODYA, Western blot and detection of biotin then Tat.

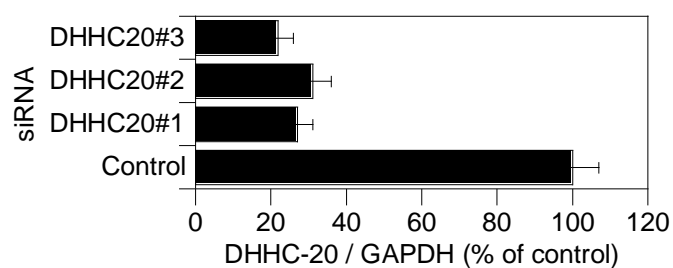
Supplementary Figure 5



Localization of DHHC enzymes in PC12 cells. Cells were transfected with the indicated GFP-tagged mouse DHHC vectors. They were then fixed and permeabilized for GM130 immunolabelling and nuclei staining using DAPI, or plasma membrane and Golgi labelling using fluorescent wheat germ agglutinin (WGA). Cells were then examined by confocal microscopy. Representative median optical sections are shown. Bar, 10 μ m.

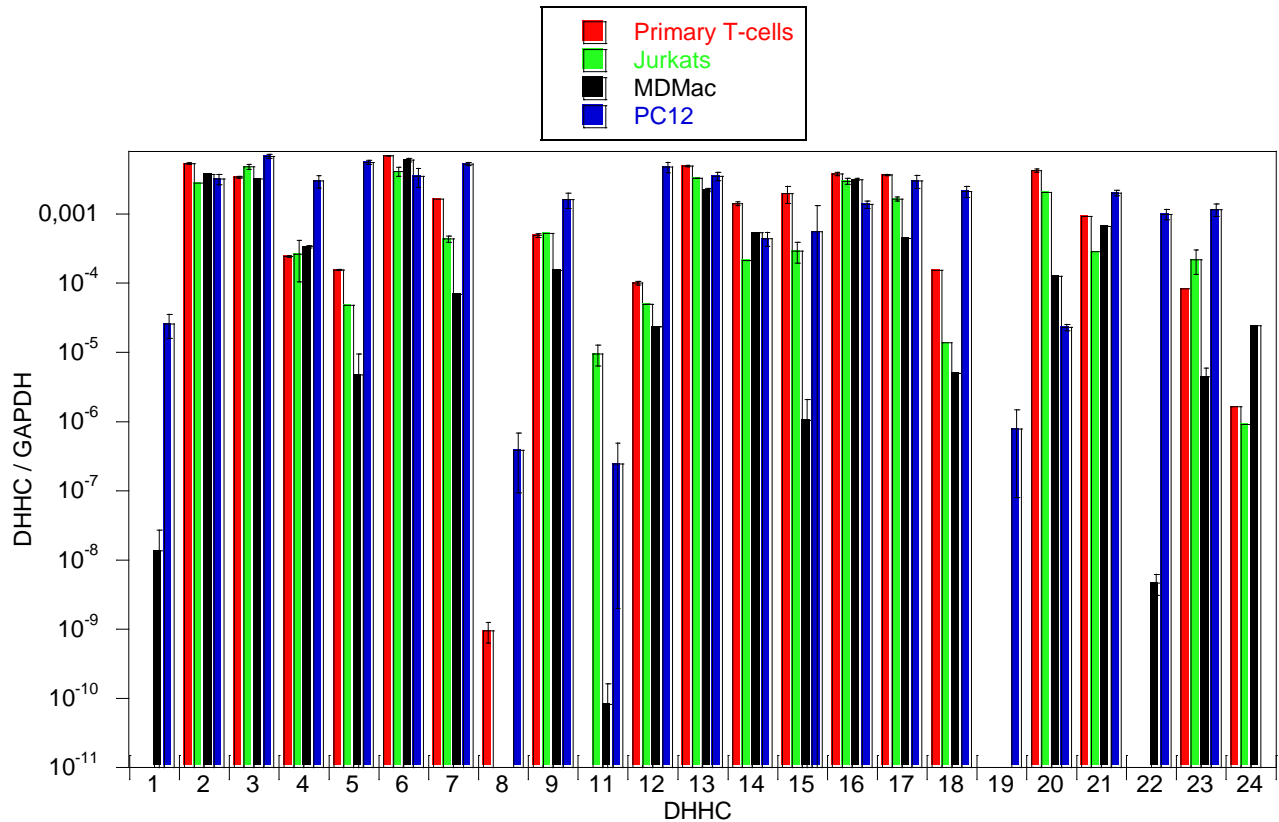


Supplementary Figure 6



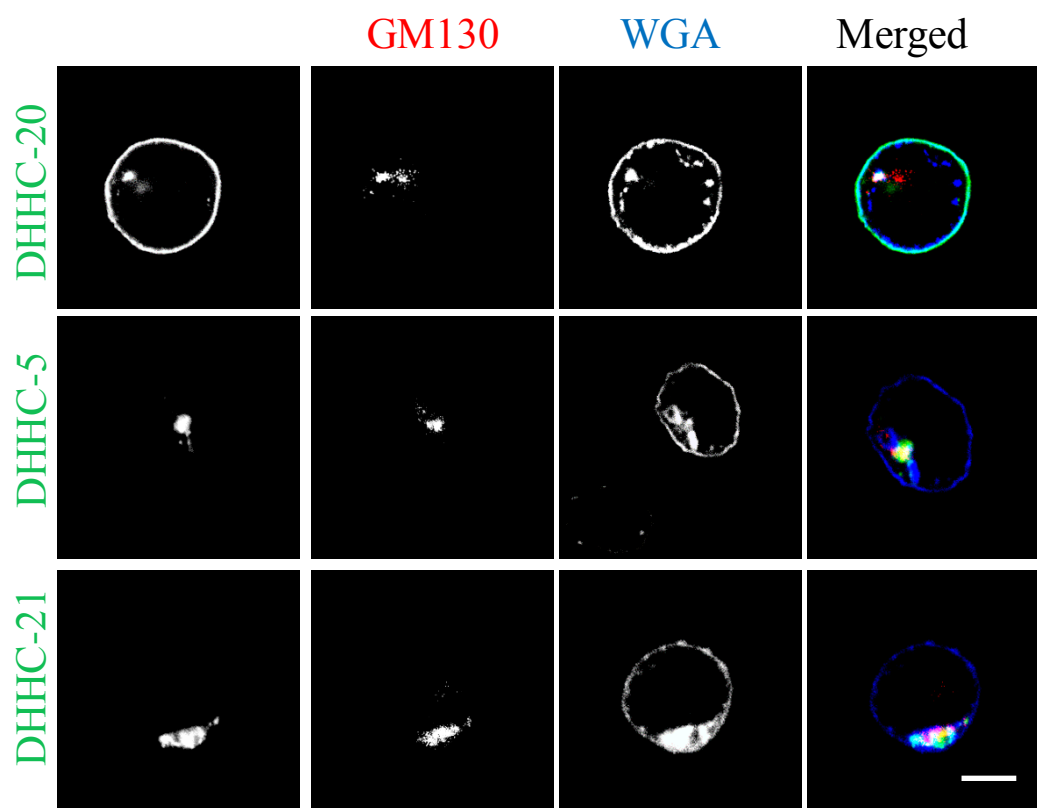
Extinction of DHHC-20 expression using siRNAs. PC12 cells were transfected with the indicated siRNA before RNA extraction and qRT-PCR to quantify DHHC-20 and GAPDH mRNAs. Results are expressed as percentages of the DHHC-20 / GAPDH control ratio. DHHC-20 siRNA #3 was used for palmitoylation experiments (Fig.3c). Means \pm SEM, n=3.

Supplementary Figure 7



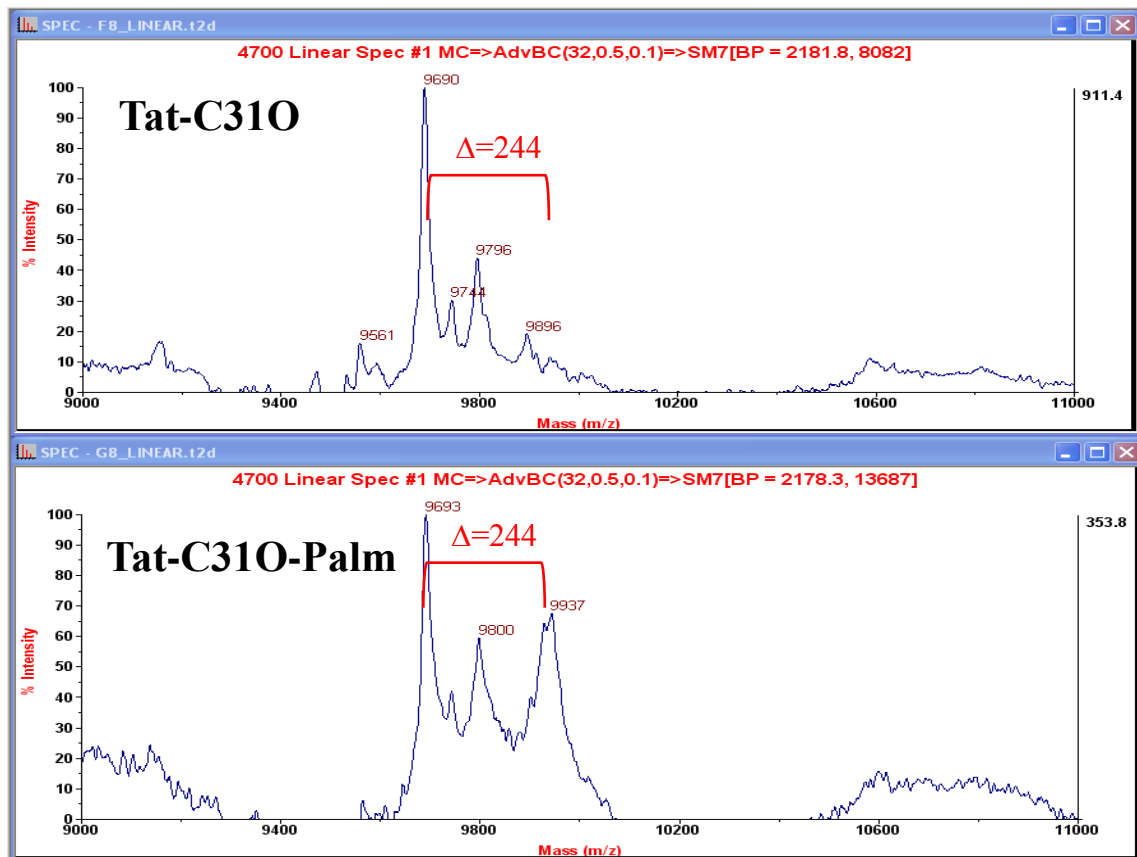
DHHC expression levels in macrophages, neuron precursors and T-cells. The RNA from monocyte-derived primary macrophages (MDMAc), PC12, Jurkat or human primary CD4⁺ T-cells was extracted before quantification of DHHCs and GAPDH mRNAs using qRT-PCR. Results are expressed as DHHC / GAPDH ratio. There are 23 DHHCs in mammals; DHHC-10 does not exist². An absent bar indicates that the corresponding DHHC was not detectable in this cell type. Means \pm SEM, n=3.

Supplementary Figure 8



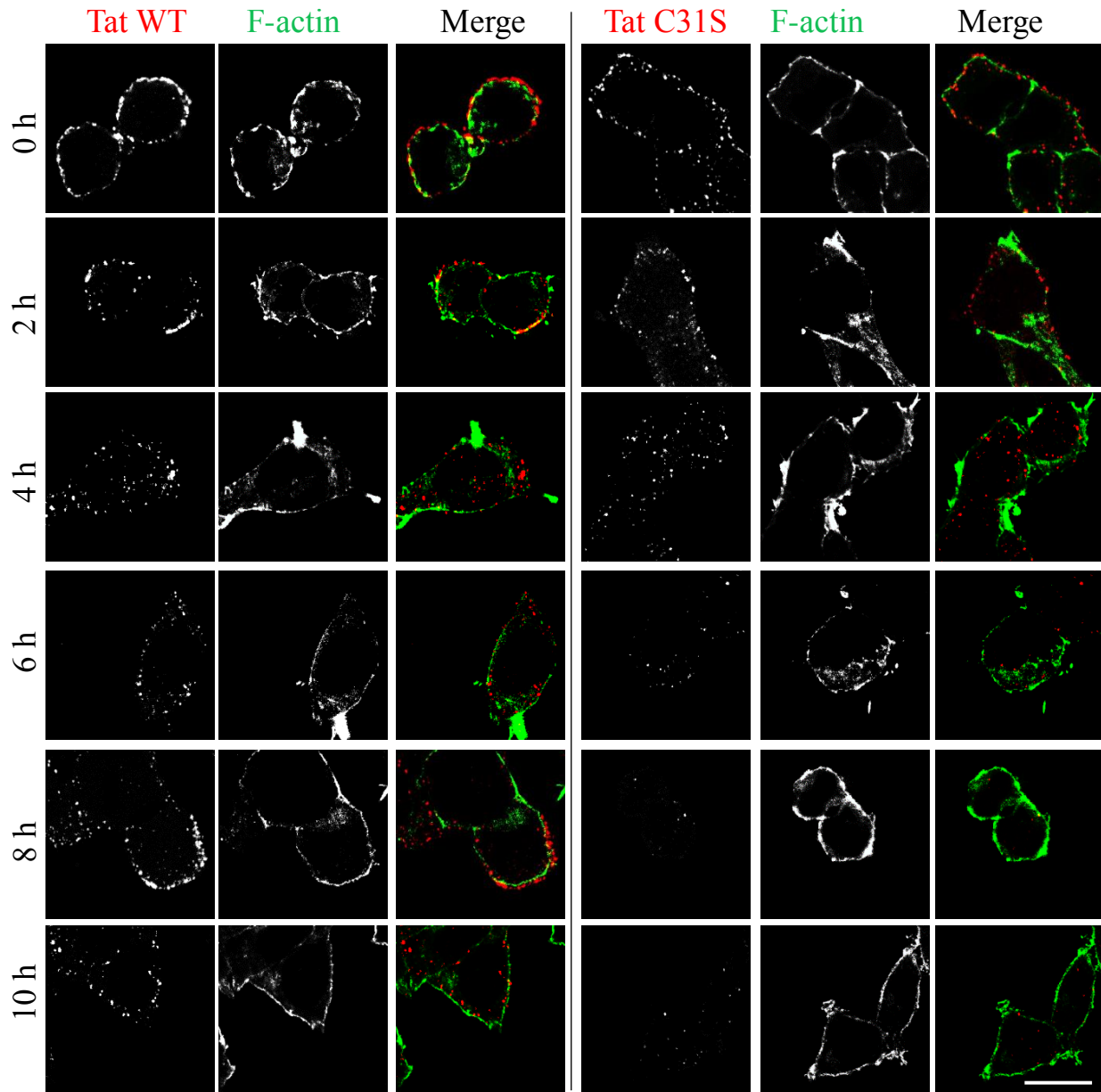
Localization of DHHC-GFP in human primary T-cells. Cells were transfected with the indicated GFP-tagged mouse DHHC enzyme then fixed and permeabilized for GM130 immunolabelling to localize the Golgi apparatus, and plasma membrane and Golgi labelling using fluorescent wheat germ agglutinin. They were then examined by confocal microscopy. Representative median optical sections are shown. Bar, 5 μ m.

Supplementary Figure 9



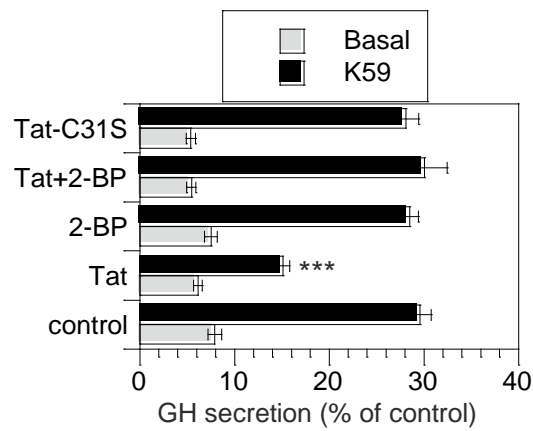
Purity and palmitoylation efficiency of Tat-C310. The theoretical MW of protonated Tat-C310 (MEPVDPRLEPWKHPGSQPKTASTNSYSKKSCFHSQVSFITKALGISYGRKKRRQRRRPPQGSQTHQVLSKQPTSQSRGDPTGPKE) is 9689. Upon palmitate addition, an H₂O is lost and a theoretical mass increase of 238 should be observed. Analysis performed using a 4800 Plus MALDI-TOF/TOF Proteomics Analyser showed that a Δ mass of 244 (± 3 Da, the precision of the instrument) is observed, confirming that Tat-C310 was palmitoylated. The peak-area ratio indicates that palmitoylation took place with an efficacy of $47 \pm 8\%$.

Supplementary Figure 10



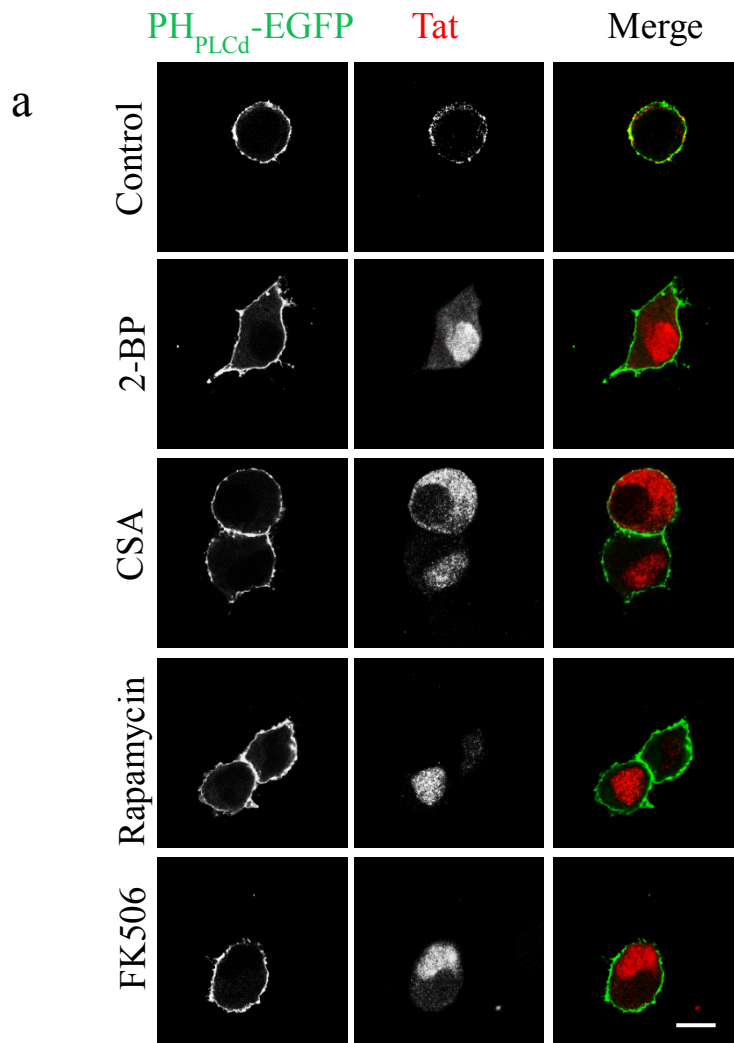
Palmitoylation is required for the recruitment at the plasma membrane of incoming Tat. PC12 cells were labeled with 100 nM Tat (WT or C31S) for 30 min at 4°C. After washing, cells were incubated at 37°C and fixed after the indicated times for Tat staining by immunofluorescence and F-actin labeling using fluorescent phalloidin. Representative median optical sections obtained with a confocal microscope are shown. Bar, 10 µm. Images from 50 < n < 100 cells were used to quantify Tat / F-actin colocalization using Manders' coefficient (Figure 4B).

Supplementary Figure 11



Palmitoylation is required for Tat to inhibit neurosecretion by chromaffin cells. Cells were transfected with human growth hormone (GH), then treated with 20 nM Tat (WT or C31S) and/or 100 μ M 2-BP for 5 h as indicated. They were then incubated for 10 min in calcium-free Locke's solution (basal release) or stimulated for 10 min with a depolarizing concentration of K^+ (K59; Locke's solution containing 59 mm KCl). GH secretion was then assayed by ELISA. Mean \pm SEM (n=3). Data were analyzed using a two-way ANOVA (***, $p < 0.001$).

Supplementary Figure 12

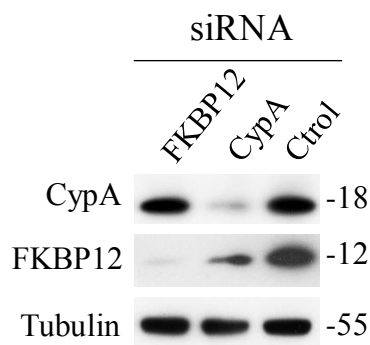


Immunophilin inhibitors displace Tat to the cytosol.

PC12 cells were cotransfected with Tat and an EGFP chimera of the PLCδ-PH. After 24 h they were treated for 5 h with the indicated drugs (100 μM 2-BP; 2 μM CSA; 1 μM rapamycin; 1 μM FK506), then washed and fixed for Tat staining by immunofluorescence.

Representative median optical sections obtained with a confocal microscope. Bar, 10 μm.

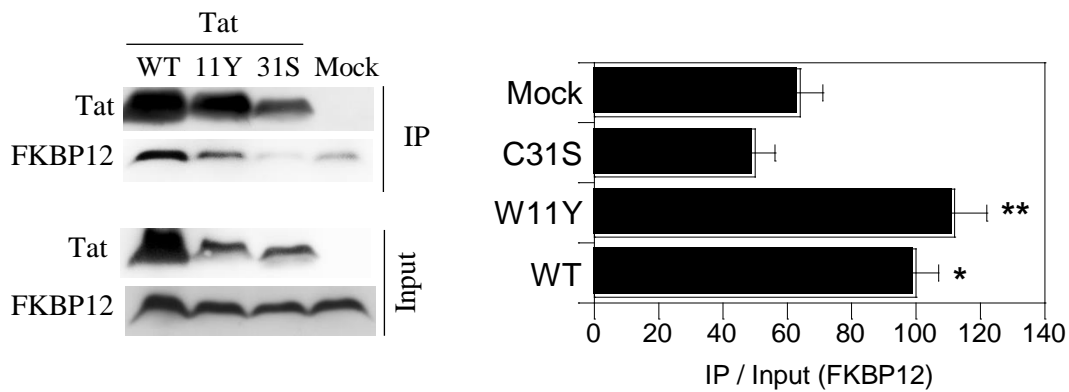
b



Silencing FKBP12 and CypA in Jurkat cells Cells were transfected with the indicated siRNA. After 24 h they were lysed for Western blotting.

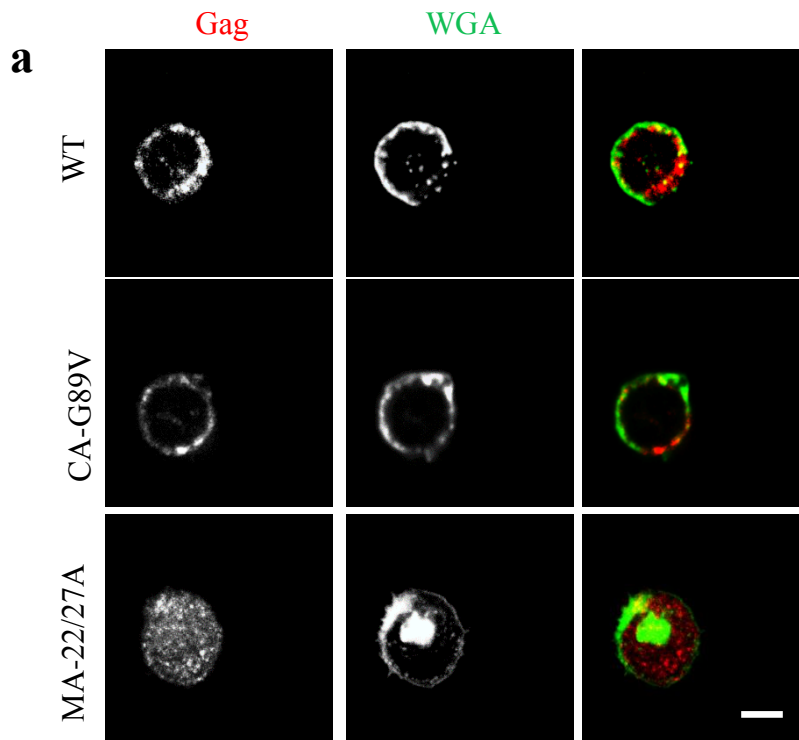
Silencing CypA also affected FKBP12 expression.

Supplementary Figure 13

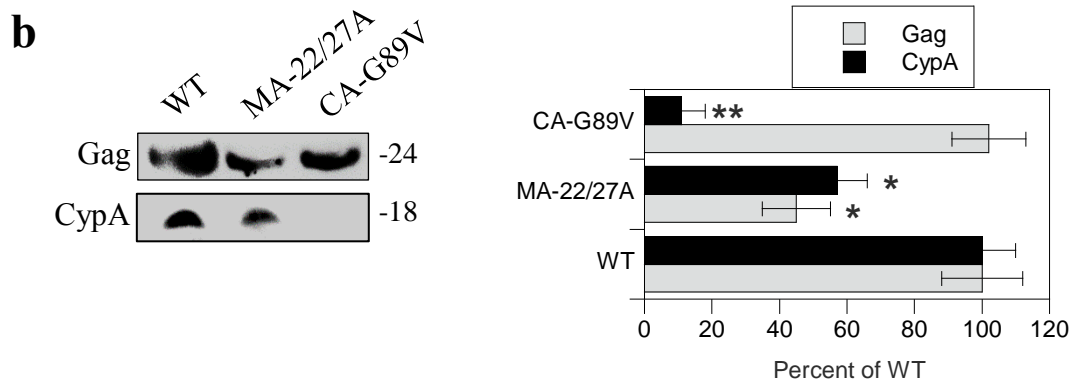


HIV-1 Tat interacts with FKBP12. HEK 293T cells were transfected with an empty vector (mock) or pBi-Tat-FLAG (WT, 11Y or C31S). Cells were lysed 24 h after transfection and Tat-FLAG was immunoprecipitated before anti-FKBP12 Western blotting. The graph shows the quantification from triplicate blots. Data (mean \pm SEM, n=3) were analysed using one-way ANOVA (**, $p < 0.01$; *, $p < 0.05$).

Supplementary Figure 14

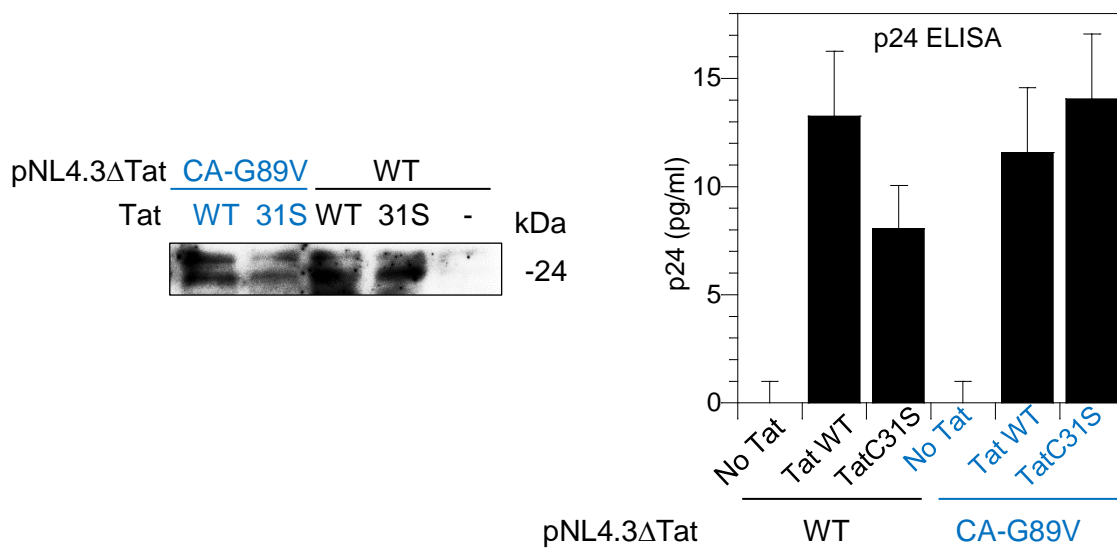


Localisation of Gag mutants in human primary T-cells. CD4⁺ primary T-cells were transfected with the indicated Gag mutant then fixed and permeabilized for p24 immunolabelling, and plasma membrane and Golgi labelling using fluorescent wheat germ agglutinin (WGA). They were then examined by confocal microscopy. Representative median optical sections are shown. Bar, 5 μ m.



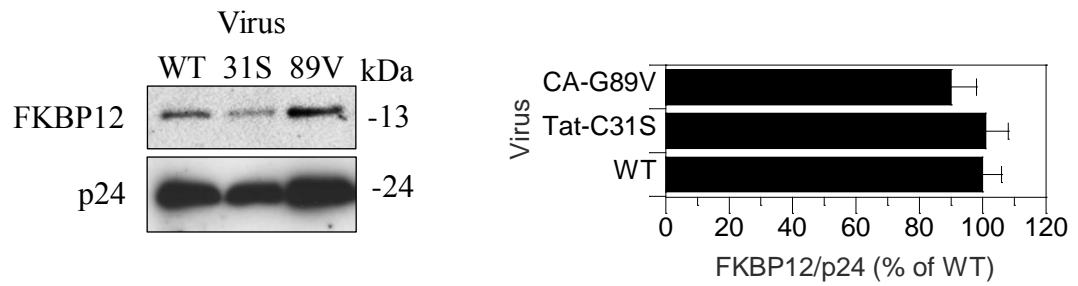
VLP production from mutant Gag proteins. Jurkat T-cells were transfected with the indicated Gag mutant; 48 h later, the medium was filtered and VLP were isolated by ultracentrifugation and analysed by western blotting. Quantification corresponds to 3 different experiments. Mean \pm s.e.m. Data were analyzed using a one way ANOVA (**, $p < 0.01$; *, $p < 0.05$).

Supplementary Figure 15



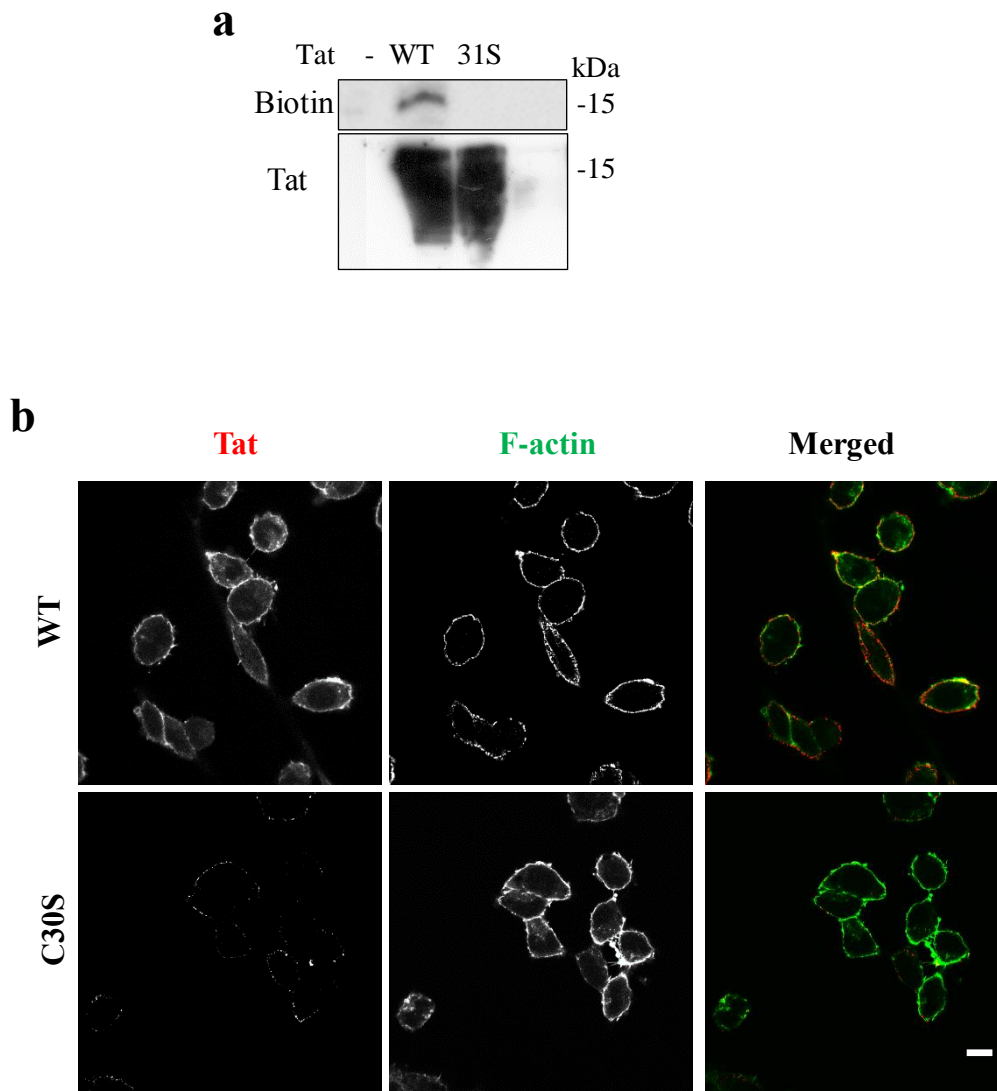
Complementation of pNL4.3ΔTat by pBi-Tat-FLAG enables virus production. HEK 293 T cells were cotransfected with pNL4.3ΔTat, WT or CA-G89V and pBi-Tat-FLAG (WT or C31S) using a ratio 4 pNL4.3 / 1 Tat. Viruses were purified from the cell medium 48 h after transfection and were analysed by SDS/PAGE and anti HIV-1 p24 Western blotting or p24 ELISA (mean \pm SEM, n=3).

Supplementary Figure 16



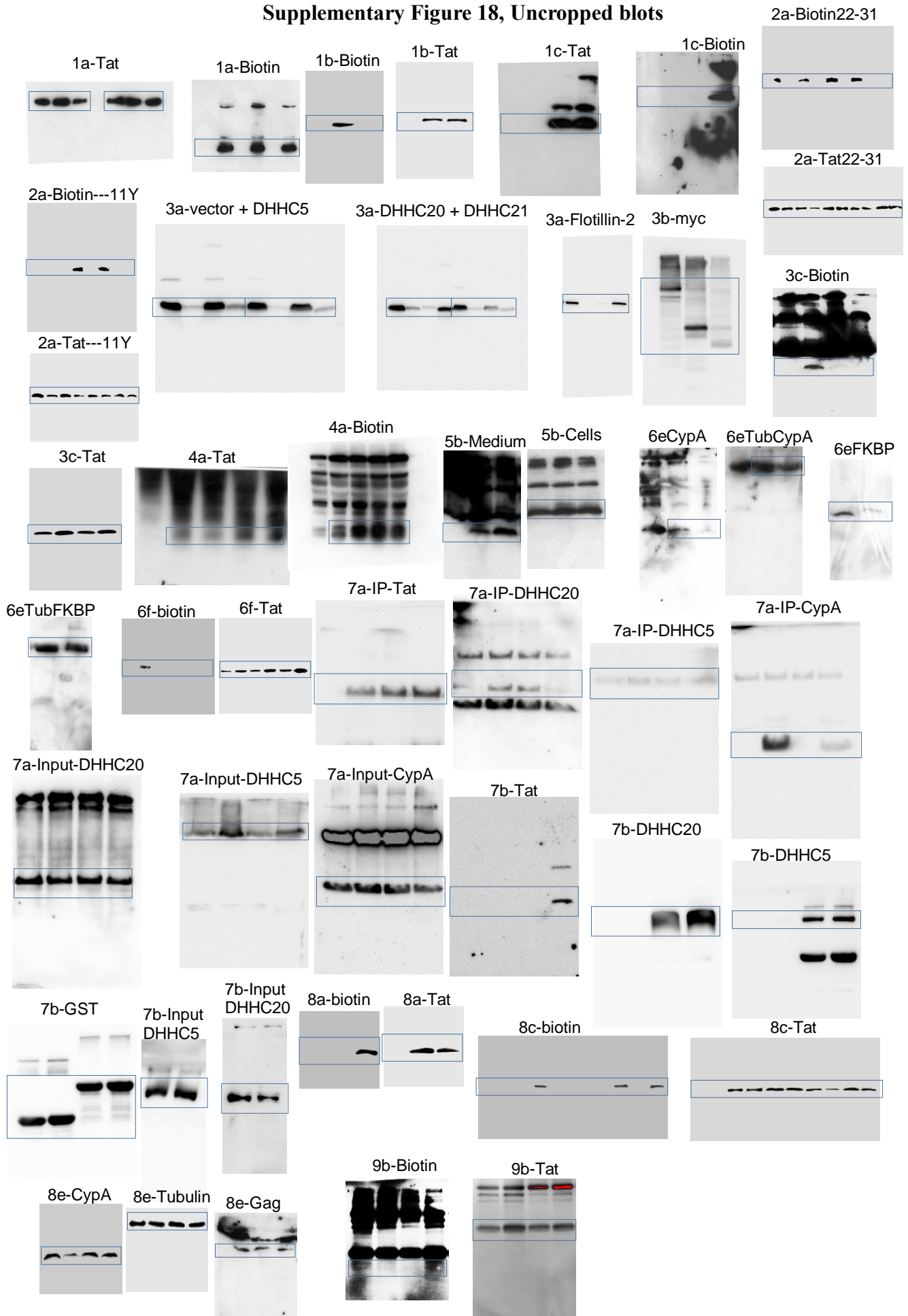
Levels of FKBP12 in WT, Tat-C31S and CA-G89V viruses. Jurkat CD4 T-cells were infected with HIV-1 (NL4.3) either WT, Tat-C31S or CA-G89V. Viruses were purified from the cell medium 48 h after infection before anti-FKBP12 and anti HIV-1 p24 Western blots. Representative experiment from n=3 experiments. The graph presents the FKBP12 levels normalized using p24 amounts (mean \pm SEM).

Supplementary Figure 17



Exogenous Tat-C30S is not palmitoylated because it is not transported to the cytosol. **a** PC12 cells were treated overnight with 100 μ M 17-ODYA and 50 nM Tat-His₆ WT, C30S, or C31S as indicated. After cell lysis, Tat-His₆ was isolated on Ni-NTA-agarose beads before click chemistry to attach biotin to 17-ODYA, Western blot and detection of biotin then Tat. WT Tat only was palmitoylated and Tat-C30S was not detectable even on overexposed blots. **b** Tat (100 nM; WT or C30S) was pre-bound to cells on ice before washes, fixation, Tat staining by immunofluorescence and imaging. Bar, 10 μ m. Quantification of 50<n<60 cells showed that the amount of cell-associated Tat-C30S was decreased by $57 \pm 3\%$ compared to WT Tat.

Supplementary Figure 18, Uncropped blots

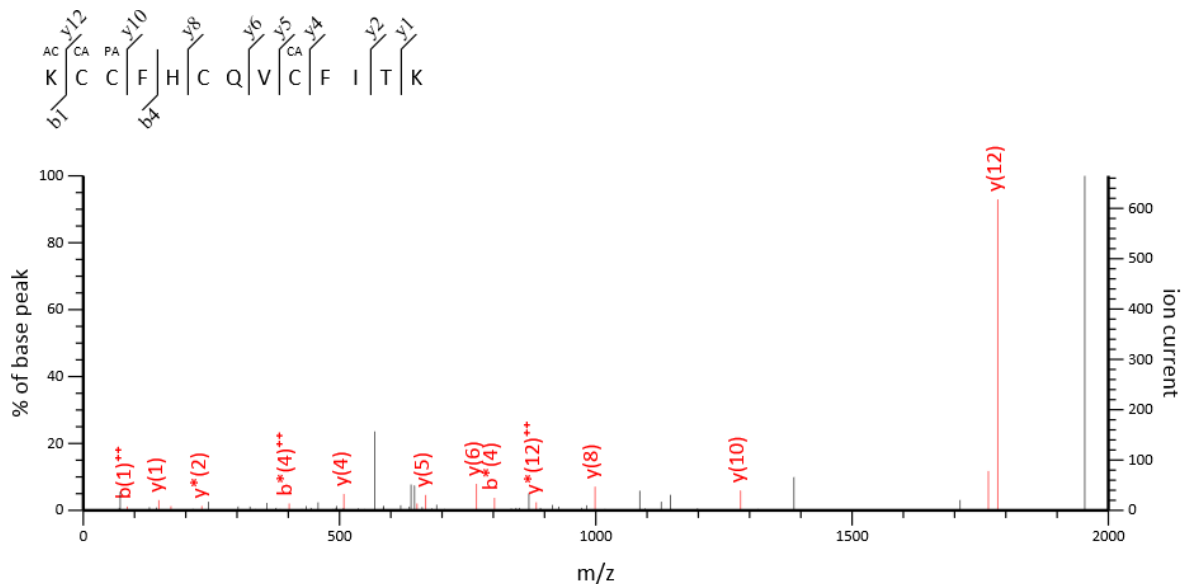


Supplementary Table 1.

B	B Ions	B+2H	B-NH3	B-H2O	AA	Y Ions	Y+2H	Y-NH3	Y-H2O	Y
1	171.1	86.1	154.1		K+42	1,954.0	977.5	1,937.0	1,936.0	13
2	331.1	166.1	314.1		C+57	1,783.9	892.4	1,766.9	1,765.9	12
3	672.4	336.7	655.4		C+238	1,623.8	812.4	1,606.8	1,605.8	11
4	819.5	410.2	802.4		F	1,282.6	641.8	1,265.6	1,264.6	10
5	956.5	478.8	939.5		H	1,135.5	568.3	1,118.5	1,117.5	9
6	1,059.5	530.3	1,042.5		C	998.5	499.7	981.5	980.5	8
7	1,187.6	594.3	1,170.6		Q	895.5	448.2	878.4	877.5	7
8	1,286.6	643.8	1,269.6		V	767.4	384.2	750.4	749.4	6
9	1,446.7	723.8	1,429.6		C+57	668.3	334.7	651.3	650.3	5
10	1,593.7	797.4	1,576.7		F	508.3	254.7	491.3	490.3	4
11	1,706.8	853.9	1,689.8		I	361.2	181.1	344.2	343.2	3
12	1,807.9	904.4	1,790.9	1,789.9	T	248.2	124.6	231.1	230.1	2
13	1,954.0	977.5	1,937.0	1,936.0	K	147.1	74.1	130.1		1

Fragmentation table of HIV-1 Tat peptide 29-41 (KCCFHCQVCFITK). PC12 cells were transfected with Tat-FLAG before immunoprecipitation using anti-FLAG antibodies, SDS/ PAGE , excision of the gel band and analysis by nano LC-MS/MS. The C+238 B and Y ions indicate that Tat is palmitoylated on Cys 31, while the others Cys are modified by carbamidomethylation (C+57 Da).

Sequence coverage (50%) includes all Cys residues and no modification of the other Cys was observed.



Fragmentation spectrum of HIV-1 Tat peptide 29-41 (KCCFHCQVCFITK)

Supplementary Table 2
DHHC primers used for real-time PCR

	For human DHHCs	For rat and mouse DHHCs
DHHC1 sense	GCGCAGCTGTTTTCAAGTCA	TTGCATGGGTGCCATCTTTG
DHHC1 antisense	CCACACACTCTTCTCAGGGG	TAGCTCTTGTCCCGCACATT
DHHC2 sense	TGGAGACAGAGCCAAGAGGAG	
DHHC2 antisense	TTATAAGTTGGCATCTGTACAGTATC	
DHHC3 sense	ACCCACCACAGTGATTCTCC	TGTCACCTGGTTTCTGGTCC
DHHC3 antisense	GTGGCCAAAACGGCTTTCA	GTCTCGGGATGGAATCAGCA
DHHC4 sense	TGTGGAACCAATCCTGGCAT	TAACCCACAGTGCTTCCAG
DHHC4 antisense	ACAGTGATGGTCGAAACGGT	TTCCGCGTAAACTAGCCCTT
DHHC5 sense	GAAGACTGAAGAAAGATAAGAGACATTC	
DHHC5 antisense	GACACTTCAAAAGTTTACTGTGGATG	
DHHC6 sense	AGCACCCTGGGTTGTATCC	GCAACCCGAGGGTTACGATA
DHHC6 antisense	ACTGTGTTCCACCCAAAGGA	TCCATCACAGGGGCACTTTT
DHHC7 sense	CAGTTCATCTCCTGTGTCCGA	CGTGGGTGAACAACTGTGTG
DHHC7 antisense	GGCTTCTCACTTTTCAATCGCT	AAGGCACAGGAAGACCAACA
DHHC8 sense	ACTCCCCACTCACCATCCTA	ATGCTCTTGTGGGAGGTGATG
DHHC8 antisense	TGCAGGTGCCAATCCGC	ACTCGGTATGCTTTGGGGTG
DHHC9 sense	GTGCTGGATCGAAGGGGTAT	GAAACTCCCGGGCAGGAATA
DHHC9 antisense	TGTCCTCCGGCATCTCATTT	ACAGCCAGATAGCGACACTC
DHHC11 sense	GTCGTTACCCCTGCACTACT	CCTCCACTCCTTTCAAGCAA
DHHC11 antisense	GGTGGAACGAGAAGATCCCC	AACATGAACACCCCAACCAT
DHHC12 sense	GTGCTCTTCTGACGATAC	GCATGGTCTGGTCTCCAGTT
DHHC12 antisense	ACATTACGTAGCCAGGGTC	GGCGATTCTGGTGTGAGGATA
DHHC13 sense	TGAAACAGACGTTGTCCCTCA	TCACTGGGCTGCCATTAAACA
DHHC13 antisense	TGTCCAATCTACCACACAGGG	CAAATGCCCTTGTCTGGATGG
DHHC14 sense	CATCGTTGGCCTCTCAGGAT	GAGGCTATATCCAGCCCGAC
DHHC14 antisense	GTCGATCAGGCTTGGTGAGA	CGCTCTGAAGTAGGGGAGTG
DHHC15 sense	TATGAATGAGTCACAGAACCCACTGCTAG	
DHHC15 antisense	TAATCTTGGTTGTCATCCTCGTTGTCTTCC	
DHHC16 sense	TGGGTGCCCTAACTGTATGG	CTAAGCCAGCACGAACACAC
DHHC16 antisense	AATACTCTGCCCTTGGCCTG	ATTGTTTAGCCAGGGGCAGT
DHHC17 sense	GGTGAACCTCTTGGACGGAA	TTACGACAACCCGTCCTTCC
DHHC17 antisense	TTTTCTTTGTCCGGTTGCCG	AGCCCAAACACCACCATACA
DHHC18 sense	CAGTGTCTGCGACAACTGTG	GGGTCCACACTTACCTCGT
DHHC18 antisense	GAAGGCCGTCAGGAATGAGA	ATGGCTGTAGGGGTTGACAG
DHHC19 sense	AGTGGCCTCTTCTTCGCATT	CAAAGTGCCTCTTCCATCGC
DHHC19 antisense	CTCAGCGGAGCCTTGATGTA	GACCGATGCAGTTGTTGACC
DHHC20 sense	ATCAACCTTTTCCTATCAAACCACTTAG	

DHHC20 antisense	GCCTTCTTCAGCTCCATTCTCC	
DHHC21 sense	TCTGGGAATTATGTAACAAGTGTAATTG	GGACCTCTTTGTTGTTTCGGC
DHHC21 antisense	AGAGCCAATGATTATCTTCACCAAC	GGAActCTCAGTGGTTGCCT
DHHC22 sense	ATGCTCTACCTCTGGTTCGC	GGCACGACCATDACTGTTTC
DHHC22 antisense	AGCCACCTCTTTCCGAAGAC	GAGATATAGGCCACTCCGGC
DHHC23 sense	TGGCTTAGGGGAGCCAAAAA	ATAAACAGCTGCGTCGGAGA
DHHC23 antisense	AGTAGTACCACAGTGCCAGC	ACGCAGGTGAAGGATAGAGC
DHHC24 sense	CTGGCTCATGTTGCTCACAG	The DHHC24 gene is absent in mouse cells.
DHHC24 antisense	GGACCCAGGTCATAGGAGTG	
GAPDH sense	ACCACGAGAAATATGACAACTCC	
GAPDH antisense	CCAAAGTTGTCATGGATGACC	

Supplementary References

1. Rayne F, *et al.* Phosphatidylinositol-(4,5)-bisphosphate enables efficient secretion of HIV-1 Tat by infected T-cells. *EMBO J* **29**, 1348-1362 (2010).
2. Greaves J, Chamberlain LH. DHHC palmitoyl transferases: substrate interactions and (patho)physiology. *Trends Biochem Sci* **36**, 245-253 (2011).